# Chapter 3 Experimental Investigation

## 3.1 Scope

In this investigation, experimental data are categorized into five groups. Each group corresponds to the particular branch combination. The group no. 1 to 5 corresponds to single, dual, triple, quadruple, and quintuple discharge condition when branches mounted on the circular surface. Dimensions of the circular surface and the branches were chosen to be geometrically similar to those of the CANDU header-feeder system.

During the experiments, the same Froude number was held at each branch line with the help of maintaing same pressure drop across the branch and adjusting the control valve positioned at each branch line.

Group nos. 1 to 5 provides the data for testing the safety codes of CANDU nuclear reactors and can show light on future research on two-phase flow distribution in headers.

## 3.2 Experimental Parameters

This section explains the geometry of branches and flow parameters for the quintuple discharge experiments. The modifications applicable to other discharge conditions are given at the end of this section.

Figure 3.1(a) shows a circular surface with total five branches, two horizontal branches B1 and B5, two inclined branches B2 and B4, and one bottom branch B3. All the five branches are of equal internal diameter d placed in the large stratified flow region of air and water at a pressure $P_{TC}$. First, B1 stream was directed to measuring phase separators (1PH) where the water flow rate $\dot{m}_{L,B1}$ was measured at the downstream. The phase separator was kept at pressure $P_{1PH}$; this created pressure drop, ΔP between the test chamber and measuring phase separator. Thus, ΔP was the pressure difference across the branch. The water level in the test chamber was kept well above B1 to prevent the gas entry into the branch. The Froude number for the B1 line calculated using equation (2.2). To obtain $Fr_L$for other branches, the above procedure was repeated with B2, B3, B4,and B5. It was observed from the experiment that the $Fr_L$ for all the five branches was same for the same ΔP condition, irrespective of their location. Therefore, $Fr_{L,B1} = Fr_{L,B2} = Fr_{L,B3} = Fr_{L,B4} = Fr_{L,B5}$.

Although, it is preferable to use five phase separators for five branches, all the branches were connected to the single phase separator i.e. auxillary phase separator (2PH) due to difficulty in maintaining more than one phase separators at a preset pressure throughout the experiment. Therefore, all the five branches were subjected to same phase separator pressure $P_{2PH}$ as shown in Figure 3.1(b).

With the above conditions, the liquid mass flow rate of five discharging streams depends upon ΔP and the location of air-water interface relative to the centre of the branches. For a fixed value of ΔP, let us consider the flow from the five branches depends on the location of the interface. In case of the high interface level above B1 and B5, the discharge from the five branches were essentially single-phase liquid with equal $Fr_L$, i.e. $Fr_{L,B1} = Fr_{L,B2} = Fr_{L,B3} = Fr_{L,B4} = Fr_{L,B5}$.

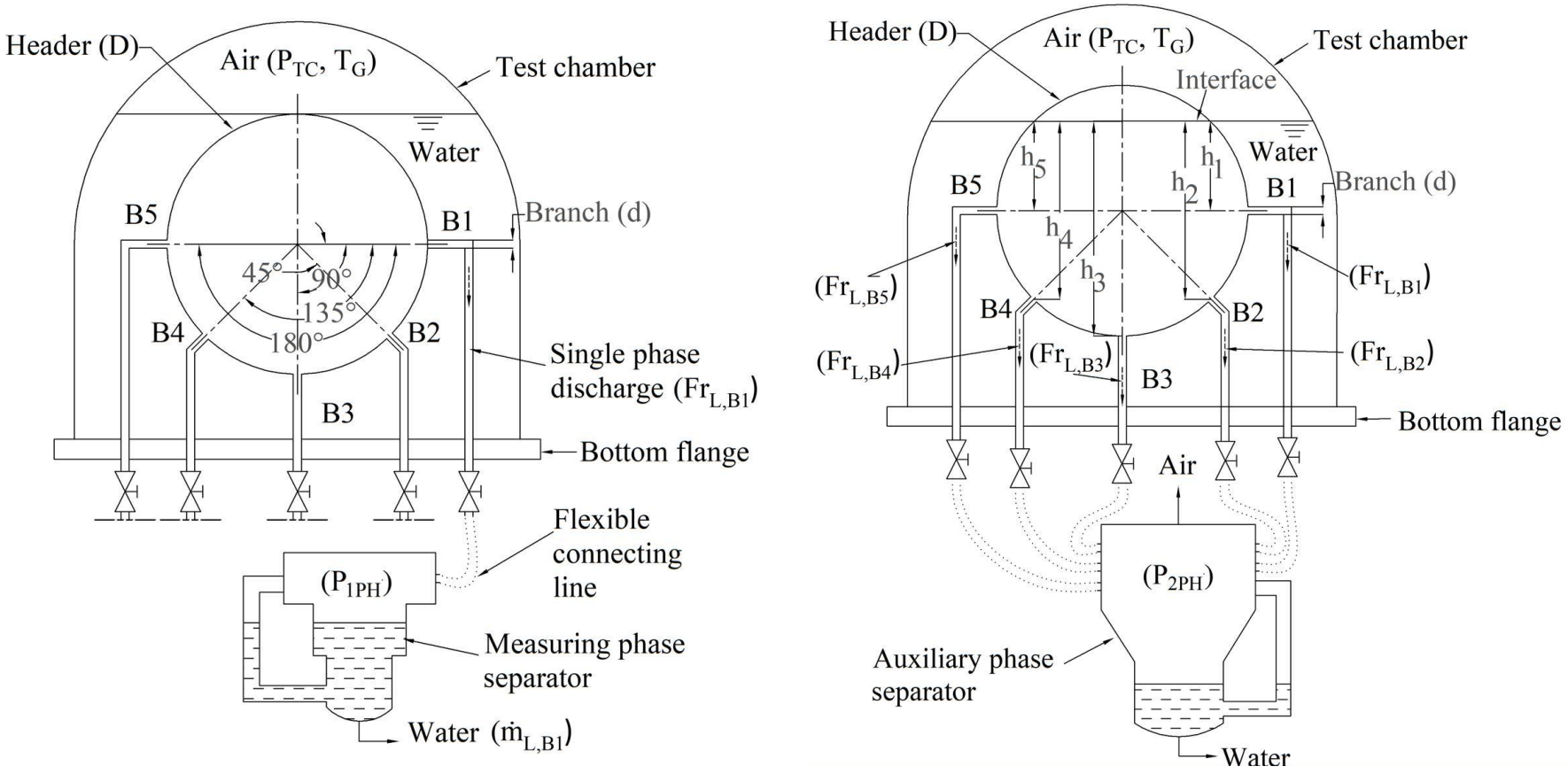


(a) Adjustment of Froude number for B1 line

(b) Parameters of OGE experiment

Figure 3.1: Experimental parameters

. As an interface level, h was lowered; a critical height was reached where OGE occurs at B1 and B5. At this moment $h_{B1} = h_{OGE,B1}$ and $h_{B5} = h_{OGE,B5}$. The $h_{OGE}$was measured from the centre of the respective branch. During OGE at B1 and B5, the gas entrainments through the branches were insignificant. Hence, quantities $Fr_{L,B1}$, $Fr_{L,B5}$, $Fr_{LOGE,B1}$ and $Fr_{LOGE,B5}$ were essentially equal. Further lowering of interface in test chamber caused a two-phase discharge at B1 and B5 while the single-phase liquid flow at B2, B3 and B4 remained unchanged. Three other OGEs $h_{OGE,B2}$, $h_{OGE,B3}$ and $h_{OGE,B4}$ at B2, B3 and B4 were encountered with further lowering of the interface. The auxiliary phase separator was kept at the same pressure that of measuring phase separator during the entire experiment. Thus the flow rates from each branch were, same as it was measured in 1PH. A study by Hassan et al. (1997) showed that at the high interface level above branches, the Froude numbers are equal from all the branches irrespective of difference in branch elevation. Besides, they also revealed that the Froude numbers before and after OGE was essentially equal as the gas entrainment through the branches were insignificant. This was found appropriate during the preliminary experiments. Therefore, $Fr_{L,B1} = Fr_{LOGE,B1}$, $Fr_{L,B2} = Fr_{LOGE,B2}$, $Fr_{L,B3} = Fr_{LOGE,B3}$, $Fr_{L,B4} = Fr_{LOGE,B4}$, and $Fr_{L,B5} = Fr_{LOGE,B5}$.

The modification in the case of single, dual, triple, and quadruple discharge experiments in group nos. 1 to 4 was one, two, three, and four active branches were directed to the auxiliary phase separator respectively and the independent parameter for OGE was $Fr_L$.

Total Six hundred and forty numbers of OGEs encountered in five groups of single and multiple discharges. Table 3.1 shows the number of OGEs encountered in each group.

Table 3.1: Number of OGEs encountered in various groups

| Group no. | Discharge condition | Series no./s. | Number of OGEs encountered |
|---|---|---|---|
| 1 | Single | 1-1 to 1-5 | 40 |
| 2 | Dual | 2-1 to 2-10 | 160 |
| 3 | Triple | 3-1 to 3-10 | 240 |
| 4 | Quadruple | 4-1 to 4-5 | 160 |
| 5 | Quintuple | 5-1 only | 40 |

The objective of this investigation was to focus on OGE and $Fr_L$ for different combinations of branches within an air-water stratified region. The experimental data were generated in a systematic fashion so that the influence of the independent parameter could be assessed.

## 3.3 Experimental Test Facility

The test facility was designed and built to investigate the influence of the independent parameters on the dependent parameter. The construction of the experimental test facility required a regulated supply of water and air, and two-phase flow separators, flow meters to measure the flow from the branches, viewing and recording facility for gas entrainment and to measure the liquid height at the onset. Figure 3.2 shows the schematic diagram of the experimental test facility. This experimental test facility consisted of a water supply system, an air supply system, a test chamber and test section, a test piece, discharge branches, and measurement systems for temperature, pressure, flow, and levevel measuring devices.

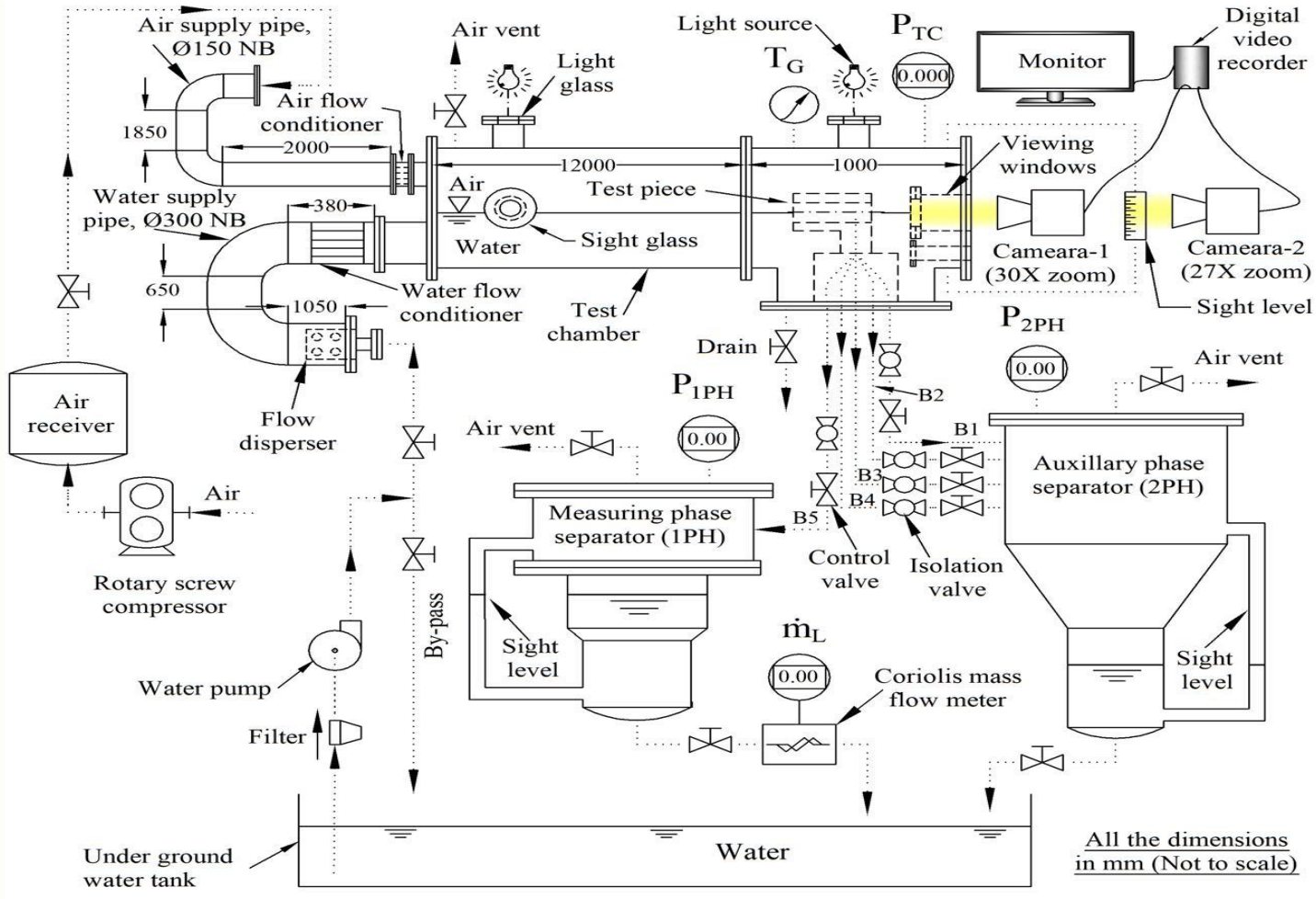


Figure 3.2: Schematic diagram of experimental set up

### 3.3.1 Water supply system

Figure 3.3 shows a schematic diagram of the water supply pipe of experimental setup. The water supplied to the flow disperser from the large underground tank using a thirteen-stage inline centrifugal pump. The pump (Make : Kirloskar Brothers Ltd., Model no.: 32 IL 13 01) could supplied the water at the rate of 5.5 $m^3$/hr at the maximum 81 meter of total head. A water flow disperser as shown in Figure 3.4 situated inside the entry of the upstream water pipe to break the water stream into a number of small streams to prevent generation of any water waves. Upstream water pipe carried water from the water flow disperser to the rear end of the test chamber passing through the water flow conditioner as shown in Figure 3.5. The water flow conditioner made of small tube inserted in the upstream water pipe to reduce the flow distortion in the water before it enters the rear end of the test chamber.

### 3.3.2 Air supply system

The screw type air compressor was used to compress the atmoshperic air and this compressed air was stored in an air receiver. The compressor (Make : Atlas Copco, Model : GA-18 AEL 11) could supplied 45.1 liters of free air per second at the maximum delivery pressure of 10.0 bar. The upstream air supply pipe as shown in Figure 3.6 carried compressed air to the rear end of the test chamber after passing through the air flow conditioner. The air flow conditioner as shwon in Figure 3.7 mounted in the upstream air pipe and near to the rear end of the test chamber was used to reduce the flow distortion in the air before it entered the rear end of the test chamber.

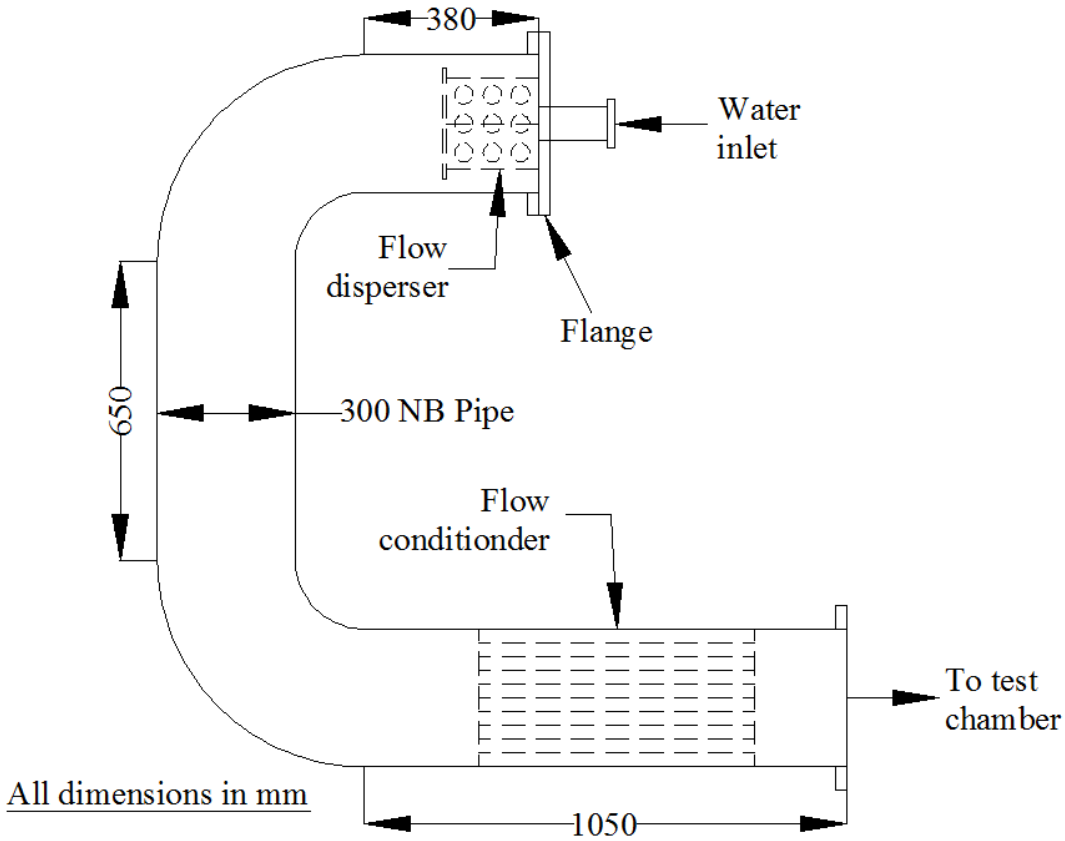


Figure 3.3: Details of the water supply pipe

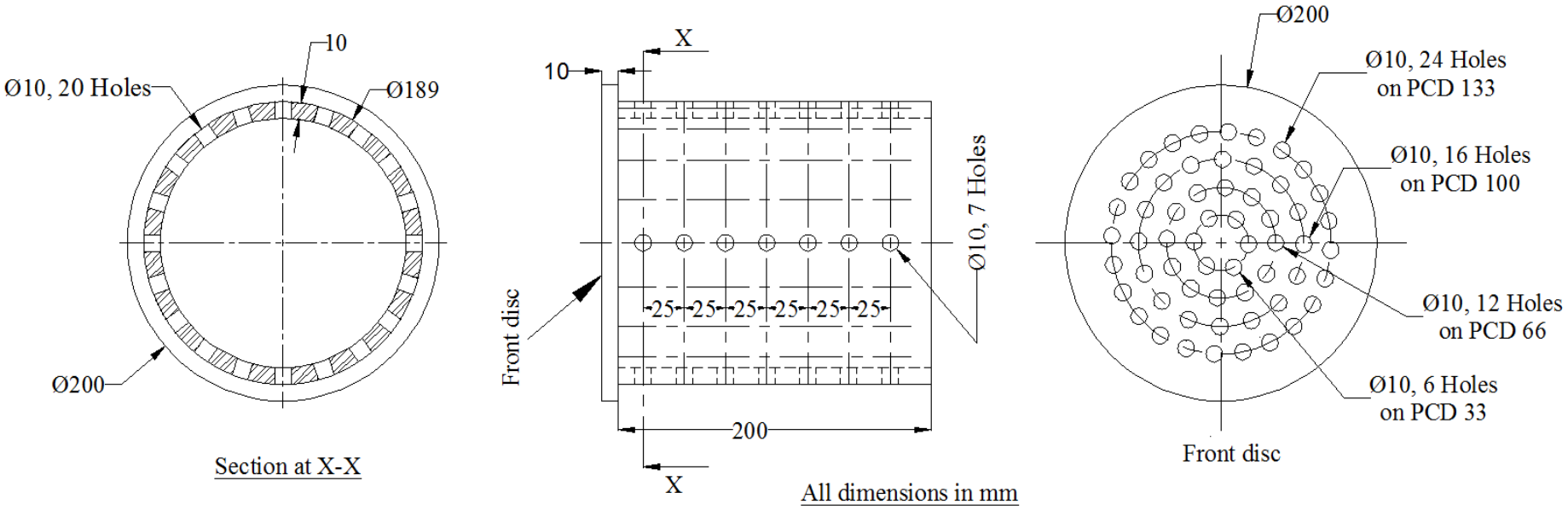


Figure 3.4: Details of the water flow disperser

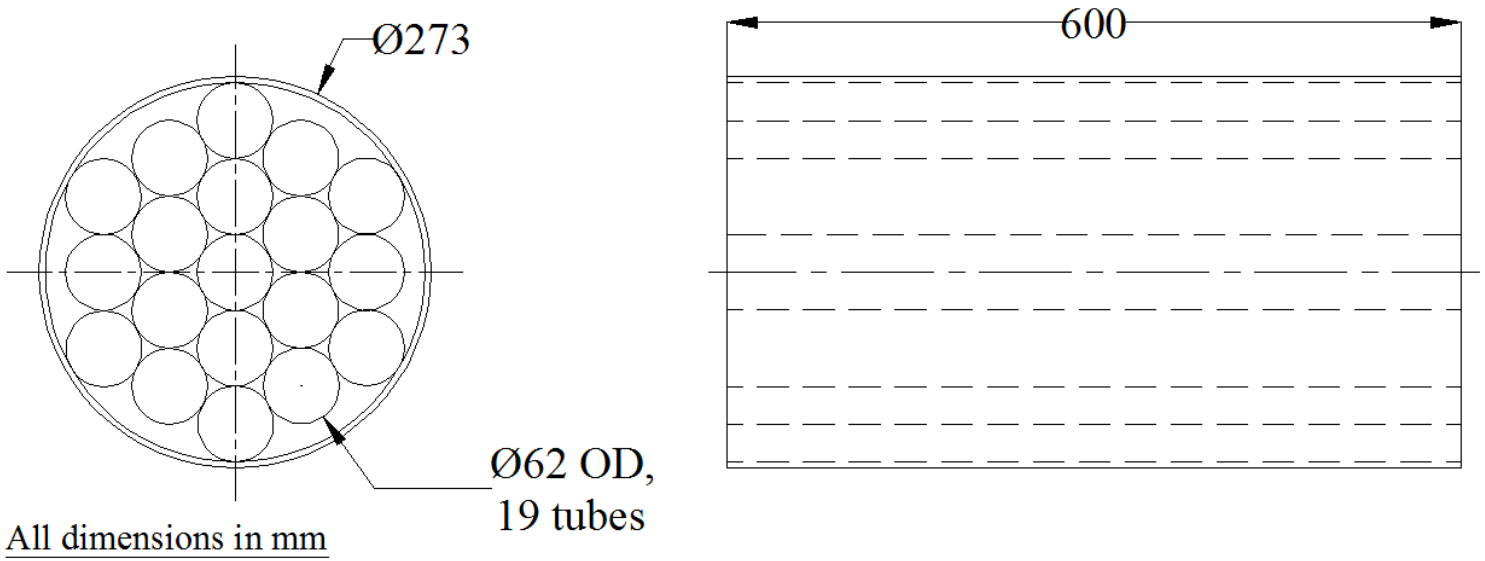


Figure 3.5: Details of the water flow conditioner

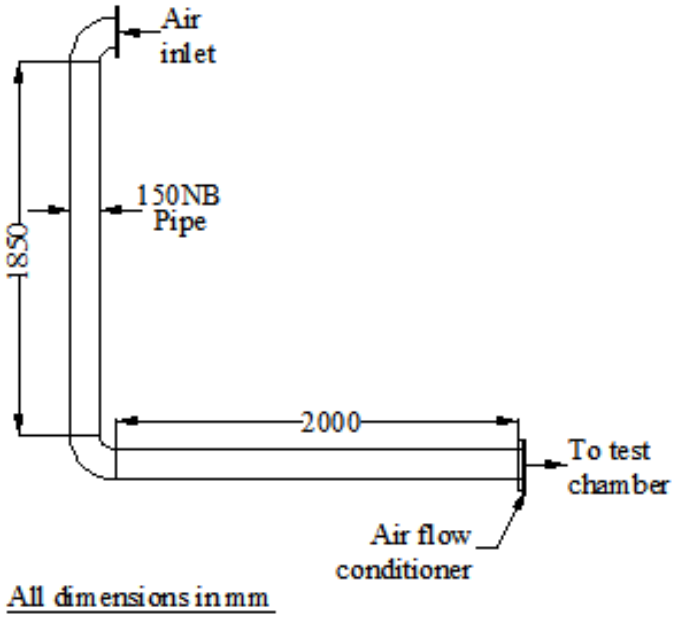


Figure 3.6: Details of the air supply pipe

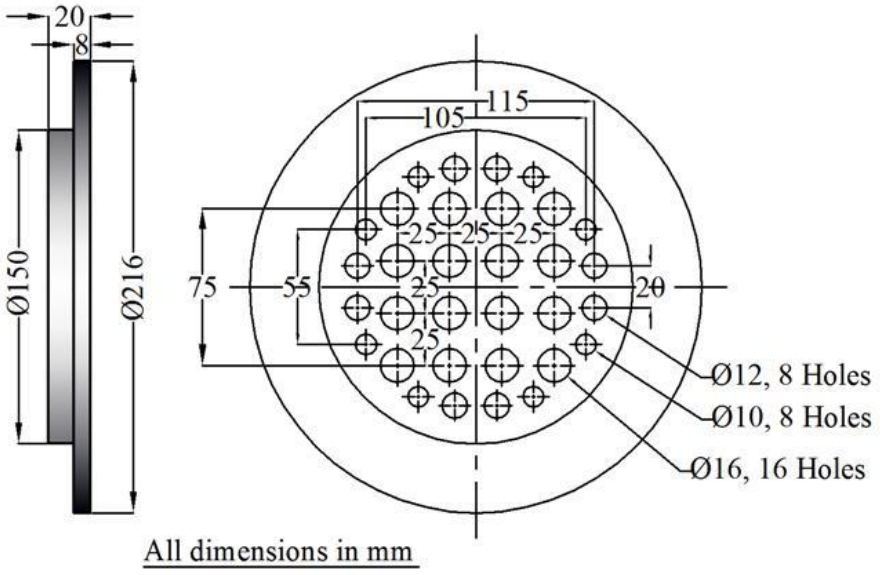


Figure 3.7: Details of the airflow conditioner

### 3.3.3 Test chamber and test section

Figure 3.8 shows the details of the test chamber with water entering though the bottom of the rear end of the chamber, while air entering from the top of the rear end of the test chamber. The test chamber of 0.6 m diameter and 11.8 m long made from carbon steel material. The other end of the test chamber connected to the T shape test section of 1.0 m in length with bottom flange on which acrylic test piece was bolted. The front end of the test section was provided by the viewing windows to view or record the vapor pull through phenomena.

### 3.3.4 Test piece

Figure 3.9 shows the schematic diagram of the acrylic test piece used for experimental work. The central hole of the test piece, 58.7 mm in diameter, represented the nuclear reactor header, while the five discharge branches, 9.0 mm in diameter represented the feeder of the nuclear reactor header. Figure 3.10 shows the image of the test piece. This test piece was bolted to the bottom flange of the test section with support structure as shown in Figure 3.11. Each branch of the test piece had a straight length of at least 17 diameters before any bends or area change was incorporated. The five branches drilled on the circular surface of the test piece at angles of $0^0$, $45^0$, $90^0$, $135^0$, and $180^0$ from the horizontal. The test piece was mounted in horizontal position by keeping the same distance between the bottom of the test piece and the top of the bottom flange of the test section at both the ends of the test piece. Thus, the data from the present test piece is representative of those for a full-header geometry of the nuclear reactor header.

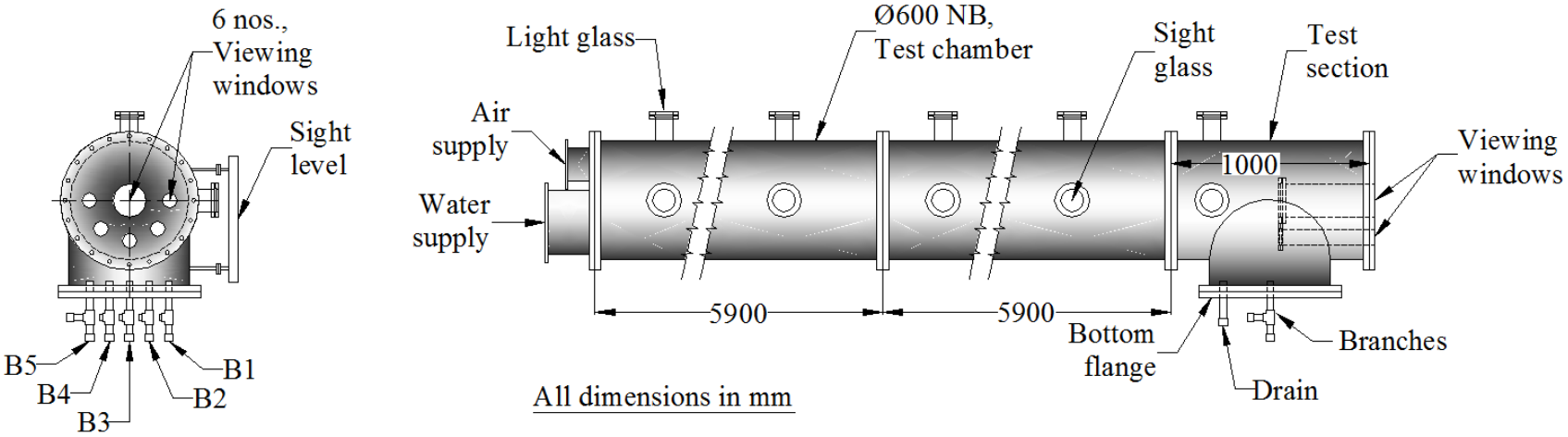


Figure 3.8: Details of the test chamber

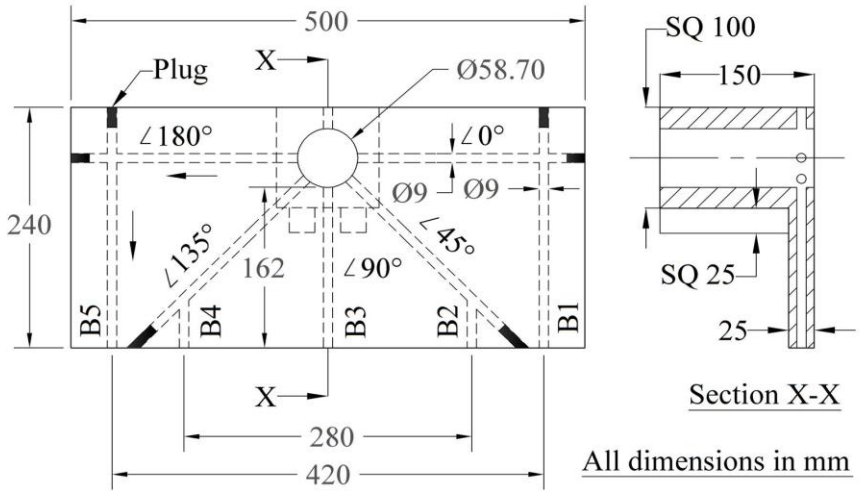


Figure 3.9: Details of the test piece

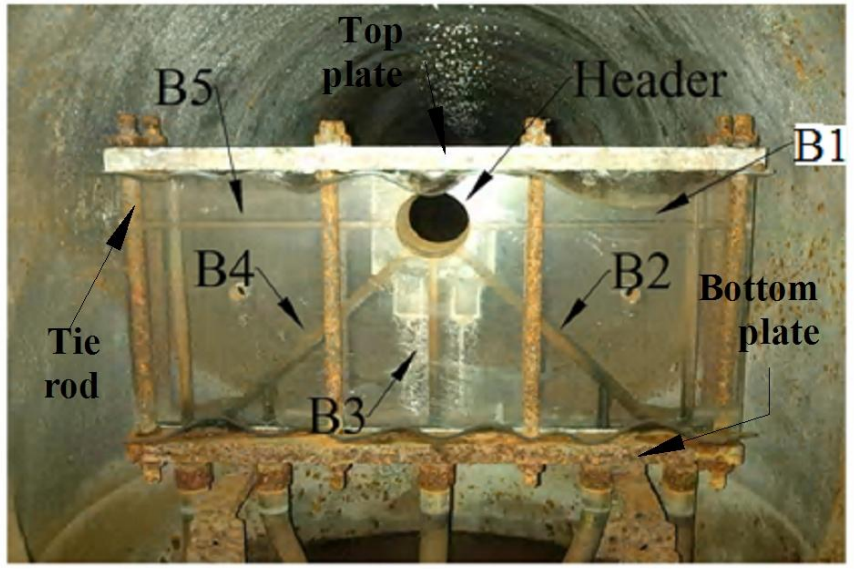


Figure 3.10: Image of the test piece

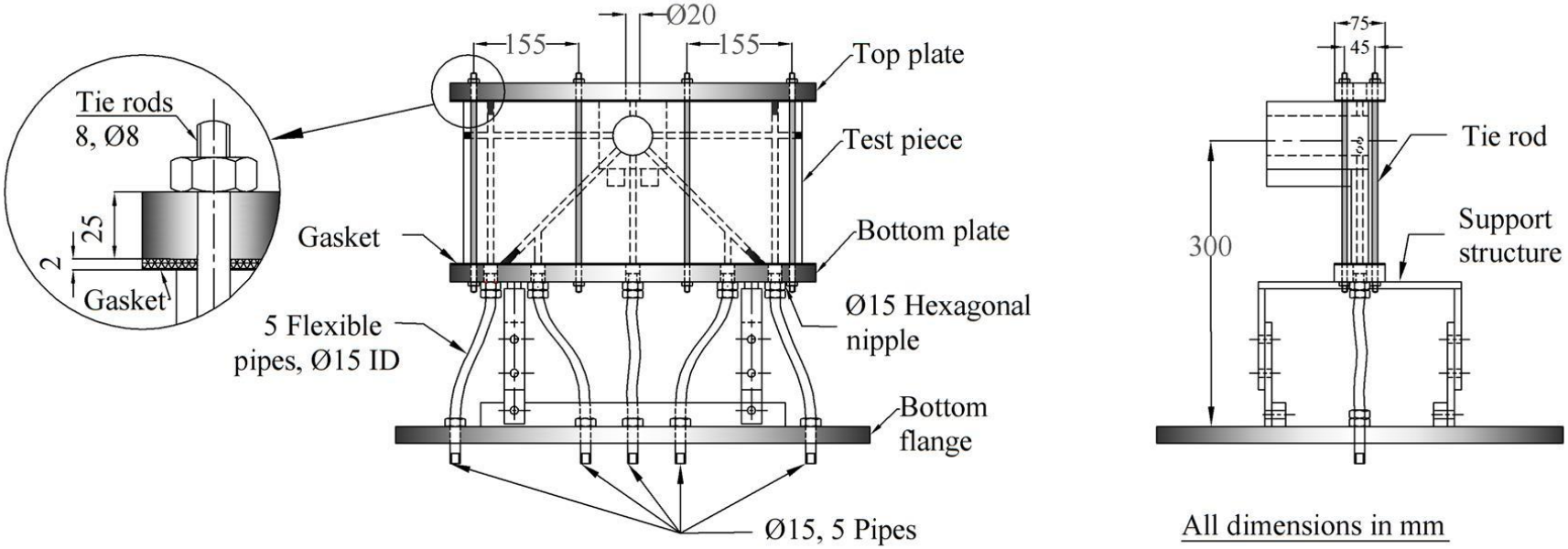


Figure 3.11: Details of the mounting of the test piece

### 3.3.5 Phase separators

Two-phase flow received from the branch lines of test piece directed to measuring phase separator (1PH) or auxiliary phase separator (2PH). Figure 3.12 and Figure 3.13 show the diagram of 1PH and 2PH respectively. Both the phase separators were designed and fabricated to split the air mass and water mass by centrifugal action. 1PH being smaller, was sensitive to air and liquid flow rates and could separate the two-phase flow received from single branch line. Liquid mass flow meter was attached to 1PH to measure the flow rate. 2PH was being bigger, could separate the two-phase flow received from five branch lines. 1PH used to adjust the equal $Fr_L$ and to calibrate branch line at different $Fr_L$. After that all the branch lines connected to 2PH to observe OGE for single and multiple discharge conditions.

1PH received the two-phase flow from the branch of the test piece header. This was attained by forcing the flow through the 15 mm inside diameter entry pipe, welded at an angle of $10^0$ in a downward direction to the separating chamber. The water exiting from the branch line flowed along the inner wall of the separating chamber and falls on the separating disc where it drained downward from the water holes. While the air exiting from the branch line flowed into a separating chamber and drained downward from the air ducts provided on the separating disc. And finally the air flowed out through the air pipe mounted at the center of the 1PH.

The bottom of the separating chamber of the 1PH was connected with pipes having two abruptly changing cross-sectional area. If the liquid flow rate from the branch was too low, the air-water interface in the 1PH was kept in the smallest diameter cross-section. On the other hand, for high liquid flow rate, the interface was

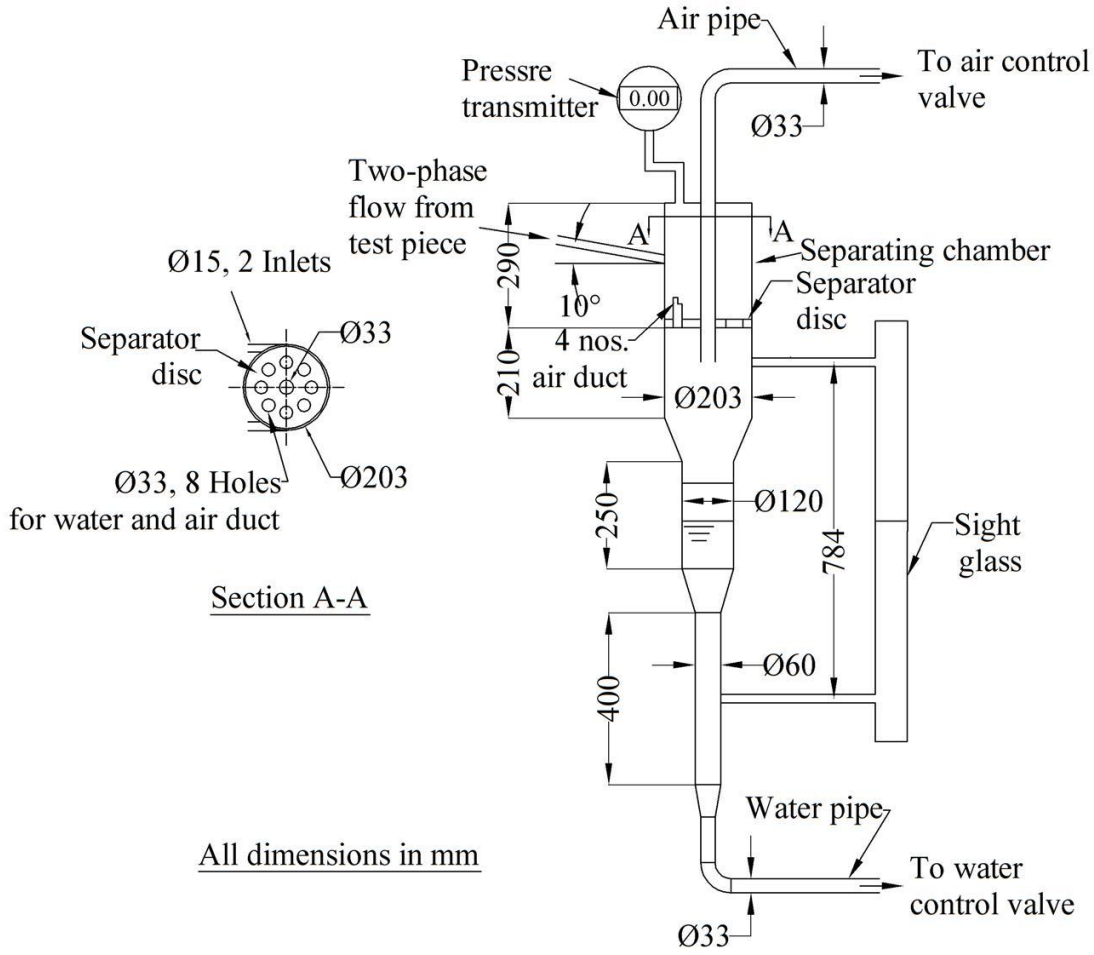


Figure 3.12: Details of the measuring phase separator (1PH)

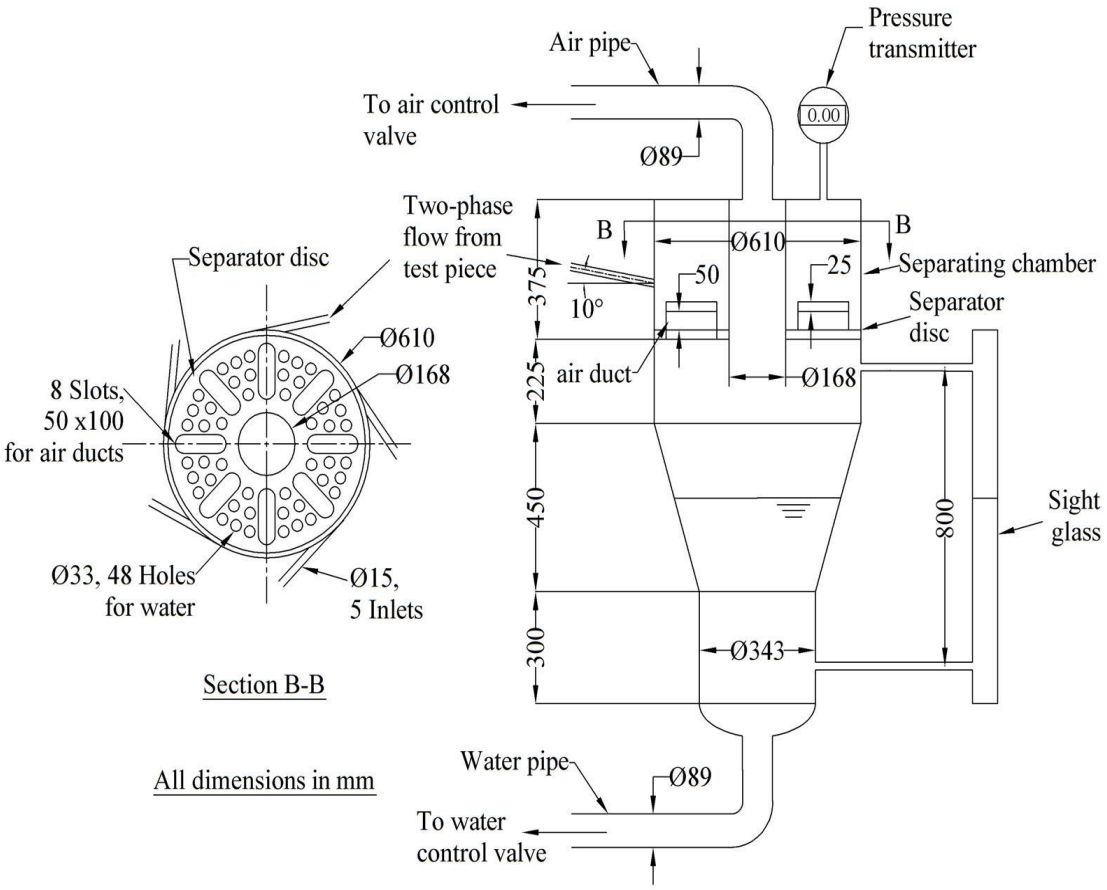


Figure 3.13: Details of the auxiliary phase separator (2PH)

kept in the middle pipe having a larger cross-section. This method reduced the errors resulting from small changes in the height of the interface with respect to time.

A glass tube liquid level indicator was installed between the smallest cross-section and separating chamber to observe the liquid level in the 1PH. A pressure tap was installed on the top flange of 1PH and connected to pressure transmitter to observe the air pressure. The reading of this pressure transmitter during experiments was monitored continuously and adjustment in outlet flow rates was made to ensure the pressure in 1PH was same.

Both the phase separators that is 1PH and 2PH, are identical in terms of the process of air pressure and liquid level control as well as separating the air mass and liquid mass. Therefore, description of 1PH is applicable to 2PH.

### 3.3.6 Liquid level measurement

A visual indication of the liquid level provided by a glass tube liquid level indicator mounted on the side of the test chamber is shown in Figure 3.14. The rise or fall of the liquid level in the test chamber resulted in a corresponding change of level in the glass tube.

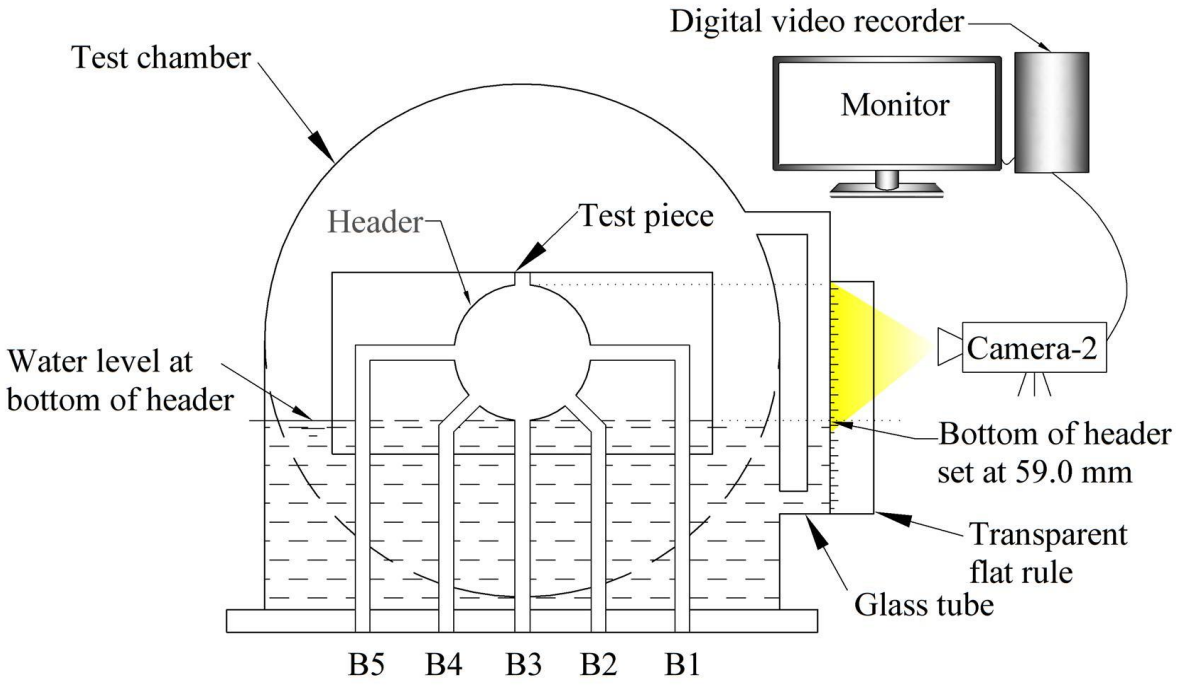


Figure 3.14: Details of liquid level measurement

To mark the bottom of the header on the glass tube, the water was pumped into the test chamber nearly 5 mm above the B3. Then, B3 was activated till all the liquid drained out from the header. At this liquid height seen in the glass tube, the bottom of the meniscus of water was at the bottom of the header and marked on it. Rotring make transparent flat ruler was attached to the glass tube to measure the liquid height in the glass tube. The flat ruler had least count of 1 mm. Therefore, The bottom of the header was marked on the glass tube aligned with the 59 mm length mark of flat ruler. This alignment was viewed on the 32 inch television screen through the camera-2 set at 14 times magnification. The image received from the camera was magnified by 200% for fine alignment between the bottom of the meniscus and the 59mm length marking on the ruler. This alignment resulted in +0.3mm systematic error in the measured liquid level in the header as the diameter of the header was 58.7mm. Therefore, from the every liquid level measurement 0.3 mm subtracted to remove this systematic error. The bevelled edge of the flat ruler had the scale marking to provide improved accuracy in reading by reducing diffraction errors.

As the liquid height is recorded and measured by camere-2 which is focused on glass tube and flat ruler, the calibration was carried out. The results of this calibration was reported in Appendix A.

### 3.3.7 Instrumentation

During the experiments, several instruments used to measure the variables. Pressure transmitter no. 1 and temperature gauge were used to measure the gauge pressure and temperature of the air in the test section. Pressure in the 1PH and 2PH measured with the help of the pressure transmitter nos. 2 and 3 respectively. These transmitters mounted on the top flange of the phase separators. In the downstream line of the 1PH, water flow measured by coriolis type mass flow meter. A globe valve used to control the flow rate through the flow meter. The details and location of the each instrument used in the experiments are listed in Table 3.2.

## 3.4 Experimental Procedure

The investigation was designed to provide quantitative assessment of the influence of $Fr_L$ at the onset of gas entrainment during various combinations of the branches, mounted on the circular surface. A data for total thirty-one series were collected in this investigation which include five series of single discharge, ten series of dual discharge, ten series of triple discharge, five series of quadruple discharge and one series of quintuple discharge. First, the experimental procedure for adjusting the Froude number and measuring the $h_{OGE}$ of branch lines during quintuple discharge condition of series no. 5-1 is discussed then changes for the single, dual, triple, and quadruple discharges are pointed out at the end of this section.

Table 3.2: Details of the various instruments used in experiment

| Instrument | Make | Model | Range | Measured variable | Location |
|---|---|---|---|---|---|
| Pressure transmitter no. 1 | Endress + Hauser | Cerabar SPMC71 : A50CB20109C | 0 to 10 bar | Gauge pressure of air in the test section | Top of the test section |
| Pressure transmitter no. 2 | Honeywell | ST 3000 : 10028809 | 0 to 10 bar | Gauge pressure of air in the measuring phase separator (1PH) | Top of the 1PH |
| Pressure transmitter no. 3 | Honeywell | ST 3000 : 10028808 | 0 to 10 bar | Gauge pressure of air in the auxiliary phase separator (2PH) | Top of the 2PH |
| Coriolis type mass flow meter | Endress + Hauser | PROMASS-83F : F90FCA2000 | 0 to 60 kg/min | Mass flow rate of outlet water from the 1PH | Water outlet line of 1PH |
| Temperature gauge | H-Guru | Mercury in steel dial thermometer | $0\ ^{0}C$ to $50\ ^{0}C$ | Temperature of air in the test section | Top of the test section |
| Aneroid barometer | - | - | 27.5 inches to 31.5 inches of mercury | Atmospheric pressure | Vicinity of test chamber |

(I) Procedure for adjustment of Froude number of branch lines;

1. First hydraulic line of B1 connected to the 1PH for adjusting the $Fr_{L,B1}$.
2. The atmospheric pressure was recorded and clean tap water pumped to a level just above the top of the header.
3. Then, air pressure was applied and kept steady in the test chamber at $P_{TC}$, and in the 1PH at $P_{1PH}$; thus the preset pressure drop across the branch, $\Delta P$, was created corresponding to the required $\dot{m}_{L,B1}$. Then control valve of the B1 was adjusted to obtain $\dot{m}_{L,B1}$ corresponding to required $Fr_{L,B1}$.
4. Under the steady $P_{TC}$ and $P_{1PH}$ Condition, the total mass of water flowed was measured in kg for not less than 180 seconds, and average $\dot{m}_{L,B1}$ was calculated. Equation 2.2 was used to calculate the average $Fr_{L,B1}$ from the average $\dot{m}_{L,B1}$.
5. A similar procedure was followed to set the equal $Fr_L$ for B2, B3, B4, and B5.

The maximum variation in setting the $Fr_L$ among the branch lines B1, B2, B3, B4 and B5 was within ±4.8 % for single and multiple discharge condition. Since the valve placed in each branch line was adjusted manually for getting equal $Fr_L$ among the branches, the variation in $Fr_L$ to this extent took place. As the the variation in $Fr_L$ among the branches reduces, the reliability of equation (2.1) generally increases. Table 3.3 shows the maximum variation in setting of $Fr_L$ in case of single and multiple discharge experiments.

Table 3.3: Maximum variation in setting of Froude number

| $Fr_L$ | Maximum variation in setting of $Fr_L$ among the five branch lines |
|---|---|
| 6.4 | 4.0% |
| 9.2 | 4.8% |
| 11.3 | 1.6% |
| 12.8 | 4.1% |
| 18.5 | 1.2% |
| 22.5 | 1.5% |
| 25.9 | 0.9% |
| 27.5 | 0.9% |

It was not possible to keep the same ΔP of measuring phase separator, in auxiliary phase separator throughout the experiment by manual valves. Therefore, the branch lines were calibrated for each $Fr_L$ for the fixed position of the control valve by slightly changing the ΔP. Appendix A gives the calibration results for the hydraulic line for each $Fr_L$.

(II) Procedure to measure $h_{OGE}$ for each test run as described below;

1. All the five branches B1, B2, B3, B4, and B5 were connected to the 2PH.
2. Clean tap water again pumped to a level just above the top edge of the test piece header.
3. The air pressure was applied and kept steady in the test chamber at $P_{TC.}$
4. The pressure in 2PH was kept the same as that of 1PH, for corresponding value of $Fr_L$. Thus, ΔP across the branch lines with 2PH was same as that of with 1PH.
5. The branch lines B1, B2, B3, B4, and B5 were activated by opening the isolation valves fitted on each branch line. Thus, water flowed through the discharge line causing a gradual drop of gas-liquid interface because of liquid flow from the active branches.
6. While keeping the steady state condition for B1 and B5, the gas-liquid interface was further lowered because of liquid flow from B2, B3, and B4. The air vent valve of 2PH was opened to release the air entered from B1 and B5 to keep steady $P_{2PH}$. At B2 and B4, the vortex free onset of gas entrainment was

visually observed on the monitor. The reading of $P_{TC}$ and $P_{2PH}$ immediately following the onset of B2 and B4 were noted.

7. The interface level was gradually dropped further because of liquid discharge from B3. The air vent valve of 2PH was further opened to release the air entered from B1, B2, B4, and B5 to keep the steady $P_{2PH}$. The reading of $P_{TC}$ and $P_{2PHH}$ immediately following the onset of B3 were noted.
8. From the recording of the camera-1, the OGE time of B1, B2, B3, B4 and B5 were noted down and the liquid height was obtained from the camera-2 at that instance of time.

For single discharge experiments of series nos. 1-1 to 1-5, the procedure was similar, except for the fact that the one branch line was directed to the auxiliary phase separator.

For dual discharge experiments of series nos. 2-1 to 2-10, two branch lines were directed to the auxiliary phase separator. In case of triple discharge experiments of series nos. 3-1 to 3-10, three branch lines, and in case of quadruple discharge experiments of series nos. 4-1 to 4-5, four branch lines were directed to the auxiliary phase separator to measure the critical height at the OGE

## 3.5 Experimental Uncertainty

An estimation of uncertainty in the independent and dependent variables was calculated as the method suggested by Moffat (1988) and Kline and McClintock (1953). The principle of uncertainty analysis is given in Appendix B. The result of the highest uncertainty analysis for each variable is given here. A summary of uncertainty analysis is provided here.

All the pressure transmitters, temperature gauge, and coriolis mass flow meters were factory calibrated. The uncertainty in $P_{TC}$ was ±1.5 percentage, in $P_{PH}$ ±1.9 percentage, in $\Delta P$ ±28.9 percentage for the smallest $Fr_L$ of 6.4 and less than ±14.8 percentage for rest of $Fr_L$. The uncertainty in $\Delta P$ decreases as $Fr_L$ increases, and at largest $Fr_L$ of 27.5 the uncertainty in $\Delta P$ was ±1.5 percentage. The uncertainty in $\dot{m}_L$ was ±2.0 percentage, and in $Fr_L$ ±2.1 percentage. The uncertainty in $T_G$ $\pm 0.5\ ^0C$ and in $h_{OGE}$ was found to be ±0.25 mm.